# Globalised scattering matrix simulations in ILC cavities and modules

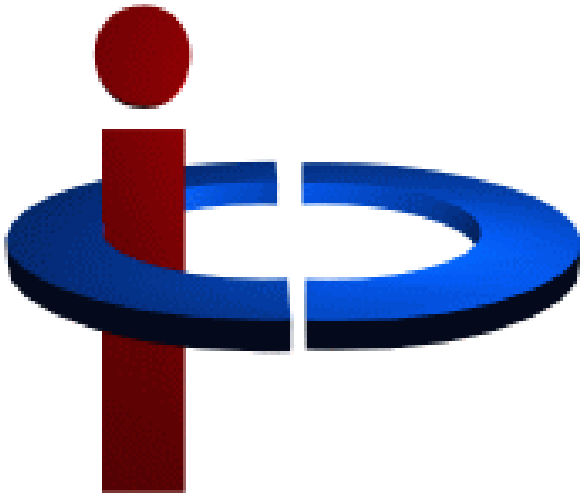


## Wakefest07 12/12/07

Ian Shinton
*The University of Manchester; Cockcroft Institute, Daresbury, UK*

# Reasons for modelling large sections of the ILC linac

- Alignment and machining errors in real modules
- Every TESLA cell will have some effect on its neighbours
- Trapped modes in various parts of the structure

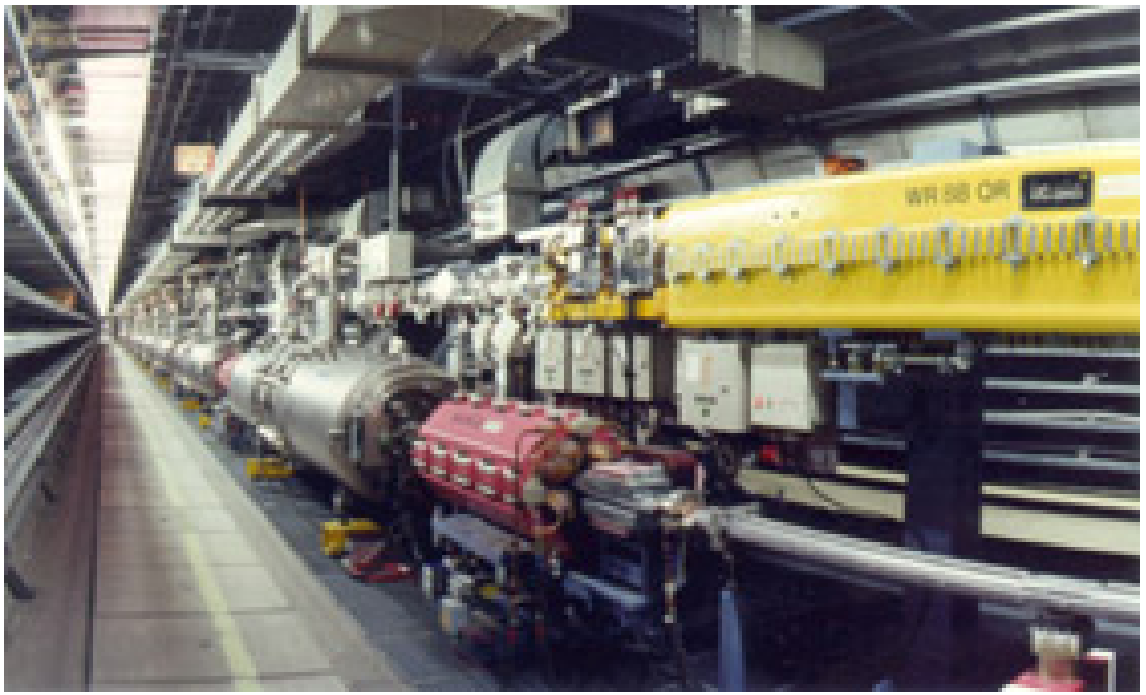

# Alignment errors and trapped modes...

A trapped mode is a resonant mode (HOM) which is non-propagating and is strongly localised in part of the accelerating structure.

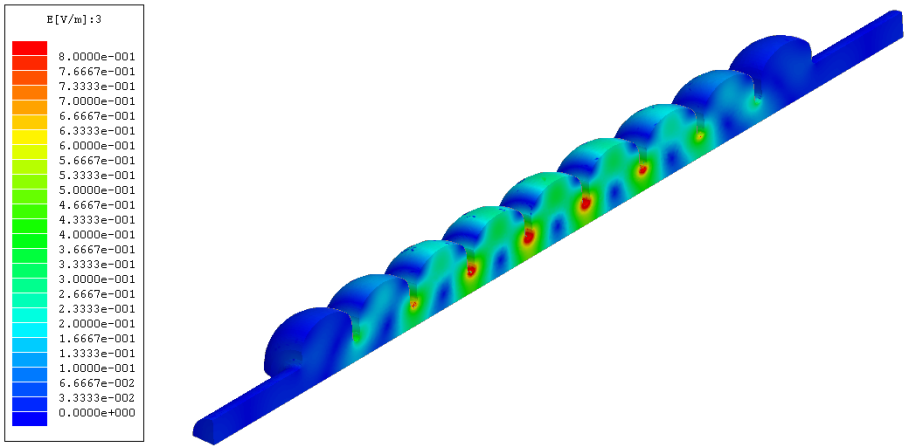


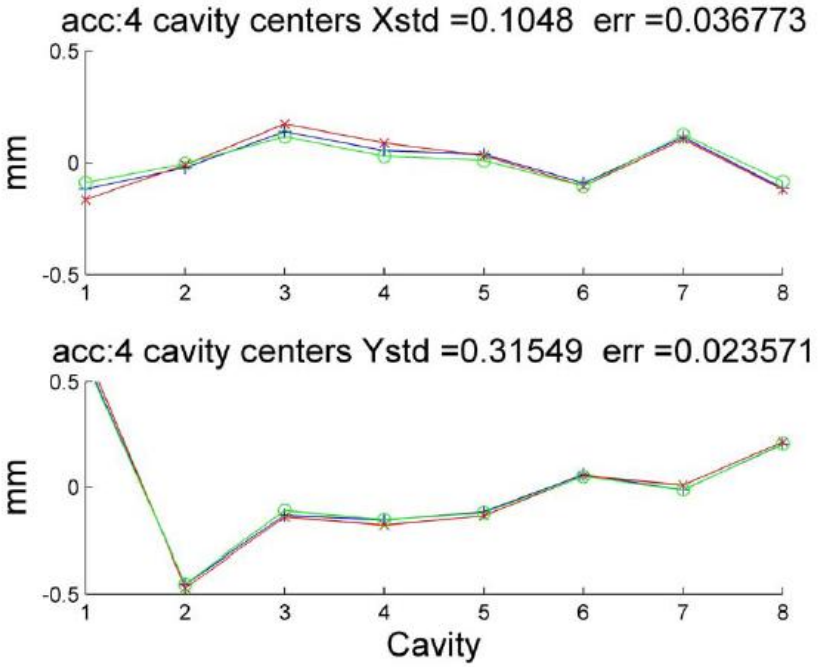


Alignment and machining errors are simply a departure away from the idealised geometry, cause by incorrect alignment or manufacture of a series of cells.

# Overall aims of the simulation effort

- Provide a realistic simulation including machining and alignment errors, to which the effect of the passage of the beam and wakefield effects can be determined
- Be able to compare the realistic simulation to experiments
- Provide a possible means by which large sections of the main ILC linacs can be accurately modelled.
- Determine the shifts in the HOM in a real structure
- Provide a means for evaluating determining positions of trapped modes, allowing couplers/cells in those regions to be tuned to avoid these modes.

# Basic cascading techniques

## Step junction cascading

All cascading techniques originate from the generalized scattering matrix technique: R.Mitra and S.W.Lee *'Analytical techniques in the theory of guided waves'*, Macmillan Comp, New York (**1971**)

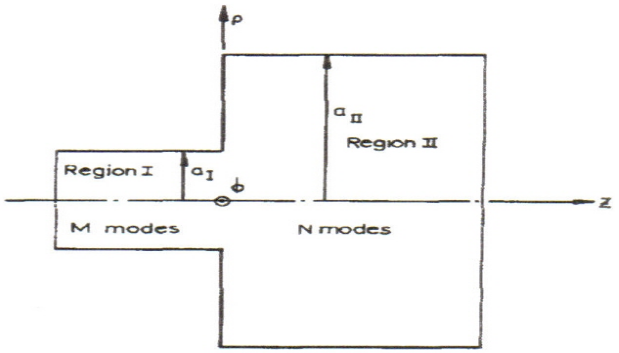


$$\underline{\underline{S}}_{11} = \underline{\underline{S}}^{a}_{12}\left[\underline{\underline{I}} - \underline{\underline{S}}^{b}_{11}\ \underline{\underline{S}}^{a}_{22}\right]^{-1}\underline{\underline{S}}^{b}_{11}\underline{\underline{S}}^{a}_{21} + \underline{\underline{S}}^{a}_{11}$$

$$\underline{\underline{S}}_{12} = \underline{\underline{S}}^{a}_{12}\left[\underline{\underline{I}} - \underline{\underline{S}}^{b}_{11}\ \underline{\underline{S}}^{a}_{22}\right]^{-1}\underline{\underline{S}}^{b}_{12}$$

$$\underline{\underline{S}}_{21} = \underline{\underline{S}}^{b}_{21}\left[\underline{\underline{I}} - \underline{\underline{S}}^{a}_{22}\ \underline{\underline{S}}^{b}_{11}\right]^{-1}\underline{\underline{S}}^{a}_{21}$$

$$\underline{\underline{S}}_{22} = \underline{\underline{S}}^{b}_{21}\left[\underline{\underline{I}} - \underline{\underline{S}}^{a}_{22}\ \underline{\underline{S}}^{b}_{11}\right]^{-1}\underline{\underline{S}}^{a}_{22}\underline{\underline{S}}^{b}_{12} + \underline{\underline{S}}^{b}_{22}$$

## Double step junction cascading

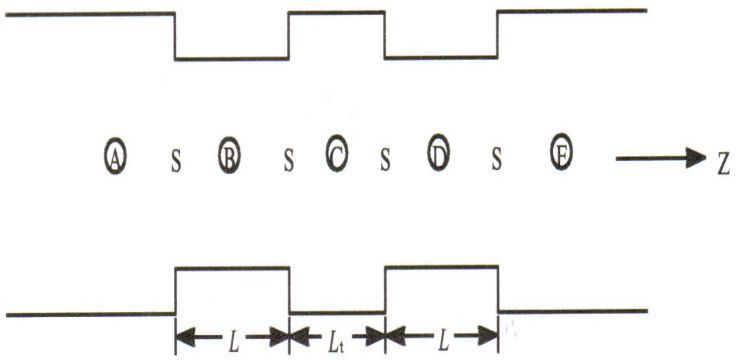


$$S_{aa} = S^{(d)}_{aa} + S^{(d)}_{ac}\,S^{(L_t)}\,U_2\,S^{(d)}_{cc}\,S^{(-L_t)}\,S^{(d)}_{ca}$$

$$S_{ae} = S^{(d)}_{ac}\,S^{(L_t)}\,U_2\,S^{(d)}_{ce}$$

$$S_{ea} = S^{(d)}_{ec}\,S^{(-L_t)}\,U_1\,S^{(d)}_{ca}$$

$$S_{ee} = S^{(d)}_{ee} + S^{(d)}_{ec}\,S^{(-L_t)}\,U_1\,S^{(d)}_{cc}\,S^{(L_t)}\,S^{(d)}_{ce}$$

$$U_1 = (I - S^{(d)}_{cc}\,S^{(L_t)}\,S^{(d)}_{cc}\,S^{(-L_t)})^{-1}$$

$$U_2 = (I - S^{(d)}_{cc}\,S^{(-L_t)}\,S^{(d)}_{cc}\,S^{(L_t)})^{-1}$$

$$S^{(-L_t)} = \begin{pmatrix} e^{-\gamma_1 L_t} & \cdots & 0 & \cdots & 0 \\ 0 & \cdots & e^{-\gamma_2 L_t} & \cdots & 0 \\ 0 & \cdots & 0 & \cdots & e^{-\gamma_n L_t} \end{pmatrix}$$

## References


R.M.Jones, N. Baboi, S.G. Tantawi, Proceedings of the 2003 Particle accelerator conference, pg 1270-1272

G.L.James, IEEE Transactions on Magnetics Vol 30, no 2, pg 1059-1066

A.K.Hamid, Int. J. Electronics Vol 80, no 3, pg 471-477

# Advantages of using a Cascading scheme

- Provided the correct physics of the problem have been considered the method is highly accurate
- The method requires little in the way of computational resources
- The method is exceedingly fast (once the unit cell calculations have been numerically obtained and catalogued)
- Perturbations and cell miss-alignments can easily be implemented into the scheme without the necessity to remesh the entire structure as would be the case in a full numerical simulation.
- Large scale simulations (of large structures) beyond the computational resources of a purely numerical approach can be made

# Things to keep in mind when cascading....

- Enough modes must be included
- The mesh used for the driven modal frequency sweep must be mesh at a high enough frequency and be of sufficient quality to obtain an accurate answer
- The propagation constant for a TESLA like structure will have some radial dependence
- "Matrix blow-up" may occur from the inversion of very small matrix terms

# Typical Cascading aspects I employ

- I use the single step junction cascading technique of G.L.James
- I consider my unit cell structures taken from iris to iris and employ a NWN cascading technique
- I have at present only considered dipole and sextupole modes
- I use HFSS to calculate the scattering matrix for my unit cell structures
- In modelling dipole modes for a TESLA like structure I have found that considering 6 modes at each port to be sufficient
- I have at present considered the frequency range from 1GHz to 4.5GHz
- I generate my mesh at or above 4.5GHz (i.e. above my range of interest), I run my simulations until they obtain an error less than 0.005%
- I assume the conductivity of Copper on all conductive surfaces

# A benchmarking Cascading example

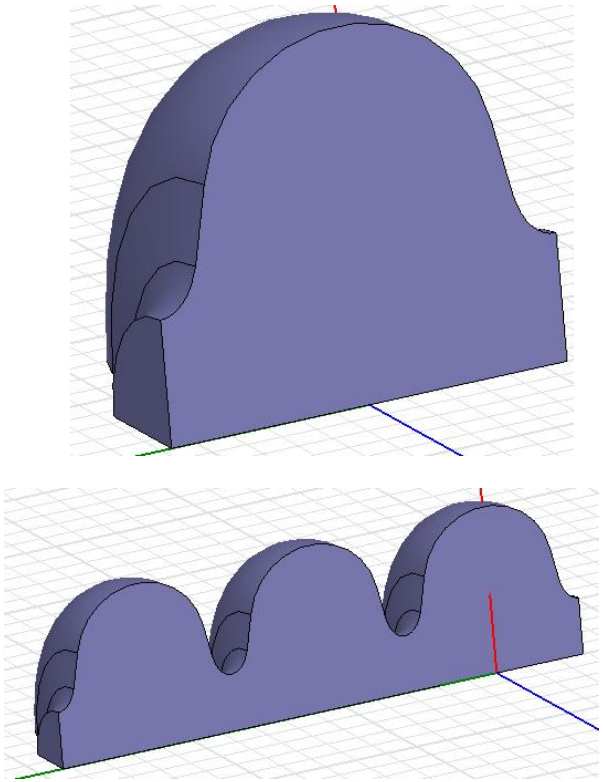

Unit cell and fully simulated structure used in benchmarking cascade calculation investigating the S21 for mode 1 (TE11) as a function of mode 1

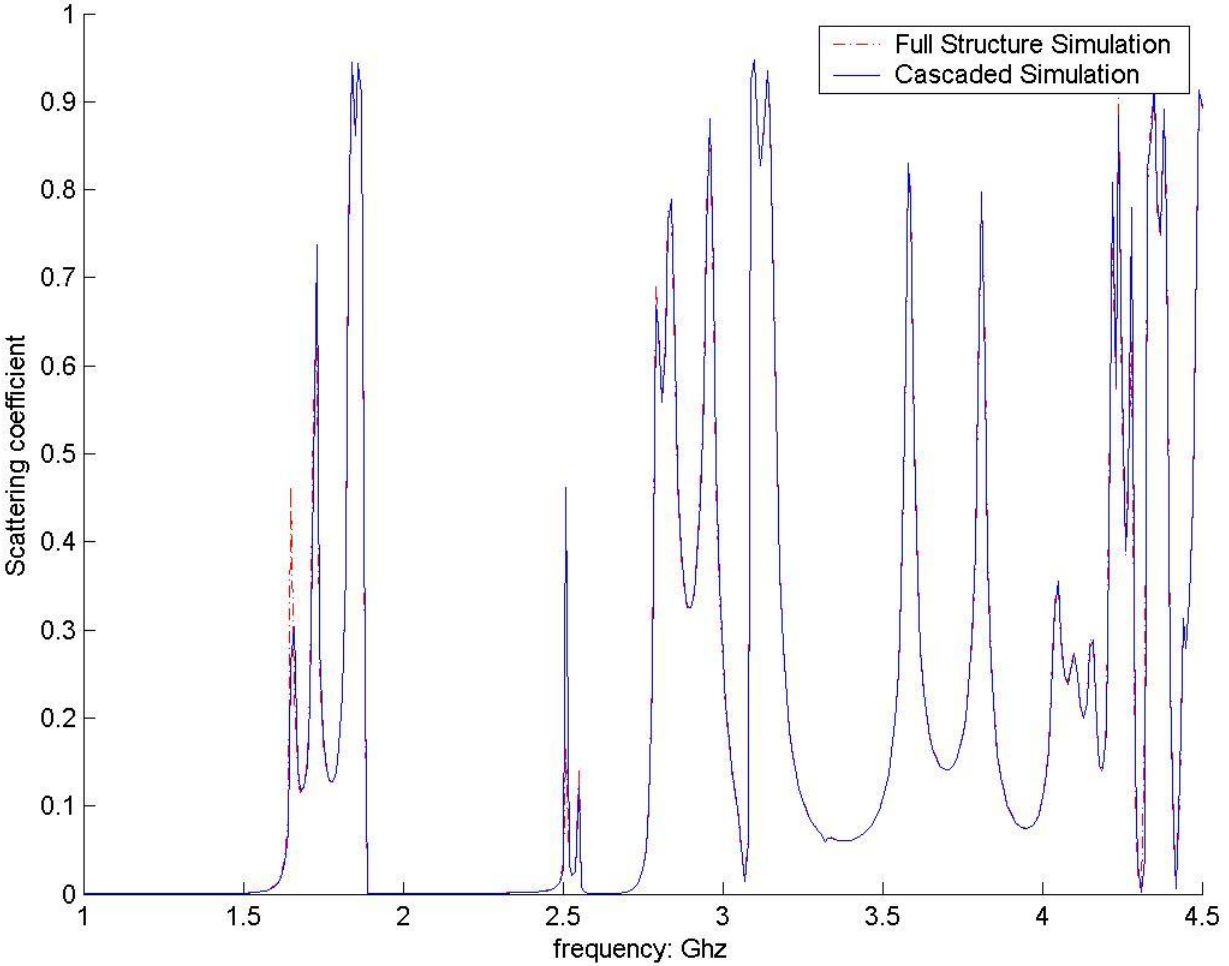


Average percentage error between cascaded and fully simulated structure was 0.014%.

Note errors below 2.5GHz are the result of meshing; however because of the later inclusion of beam pipes this aspect is a mute one. The cascading calculation took 1.3 seconds while the full numerical HFSS equivalent simulation took about 1 day

# The accuracy of a Cascading scheme for large structures

- Power conservation
- Lets consider a structure comprising solely of identical middle cells (no beam pipes) – lets consider the structure to be 100m in length as a benchmark problem. The GSM compilation error initiated from any cell in the structure is less than $5x10^{-3}$

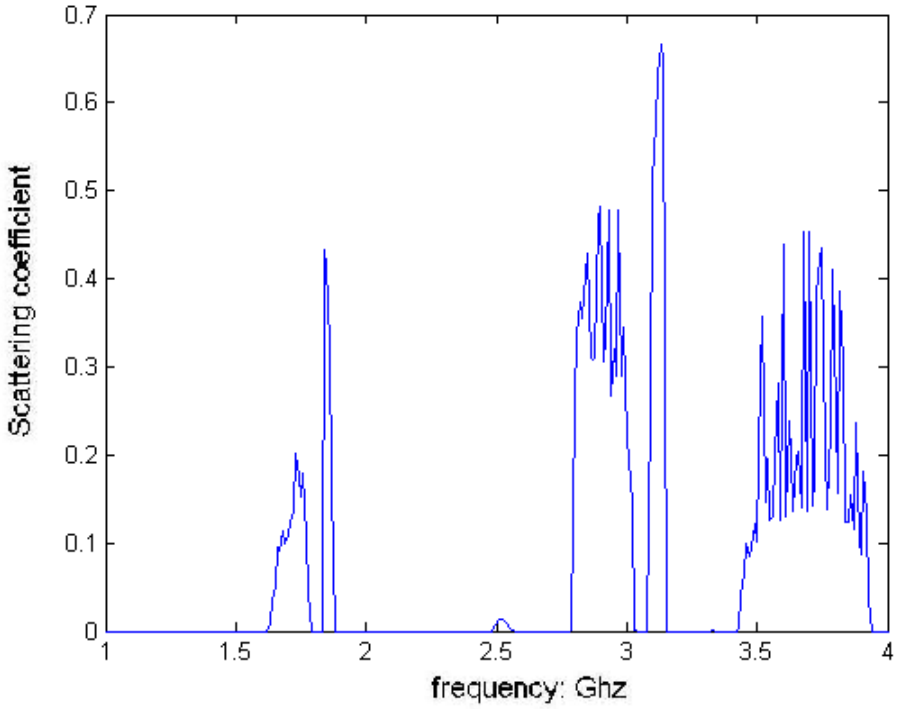


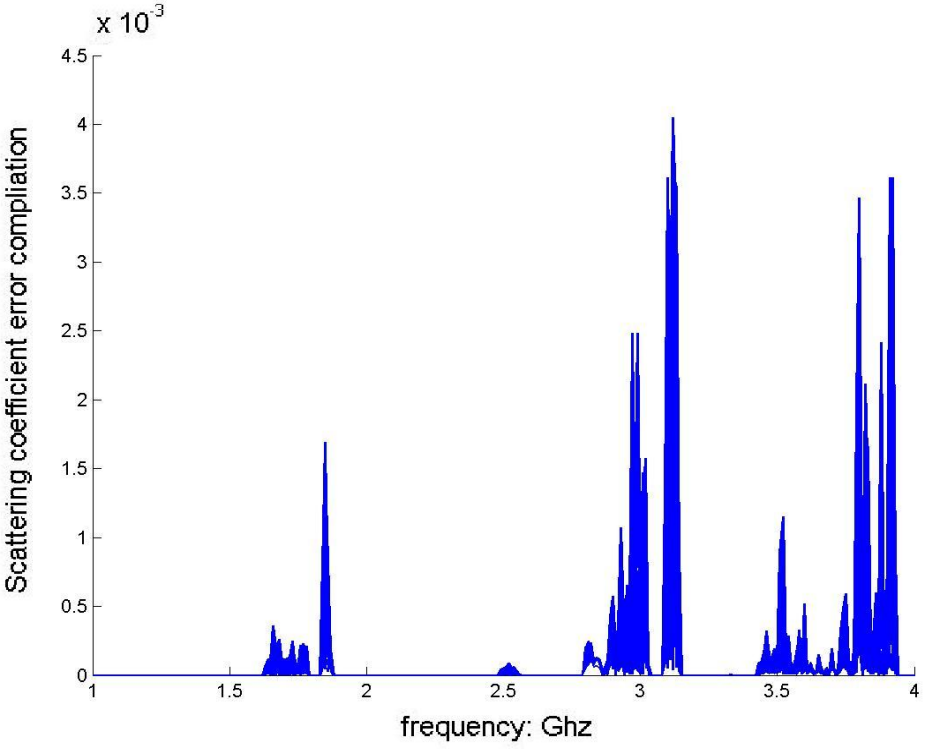

# Comparison of the S21 matrix for 7 cascaded middle cells of the three cavity designs for mode 1 (TE11) as a function of mode 1

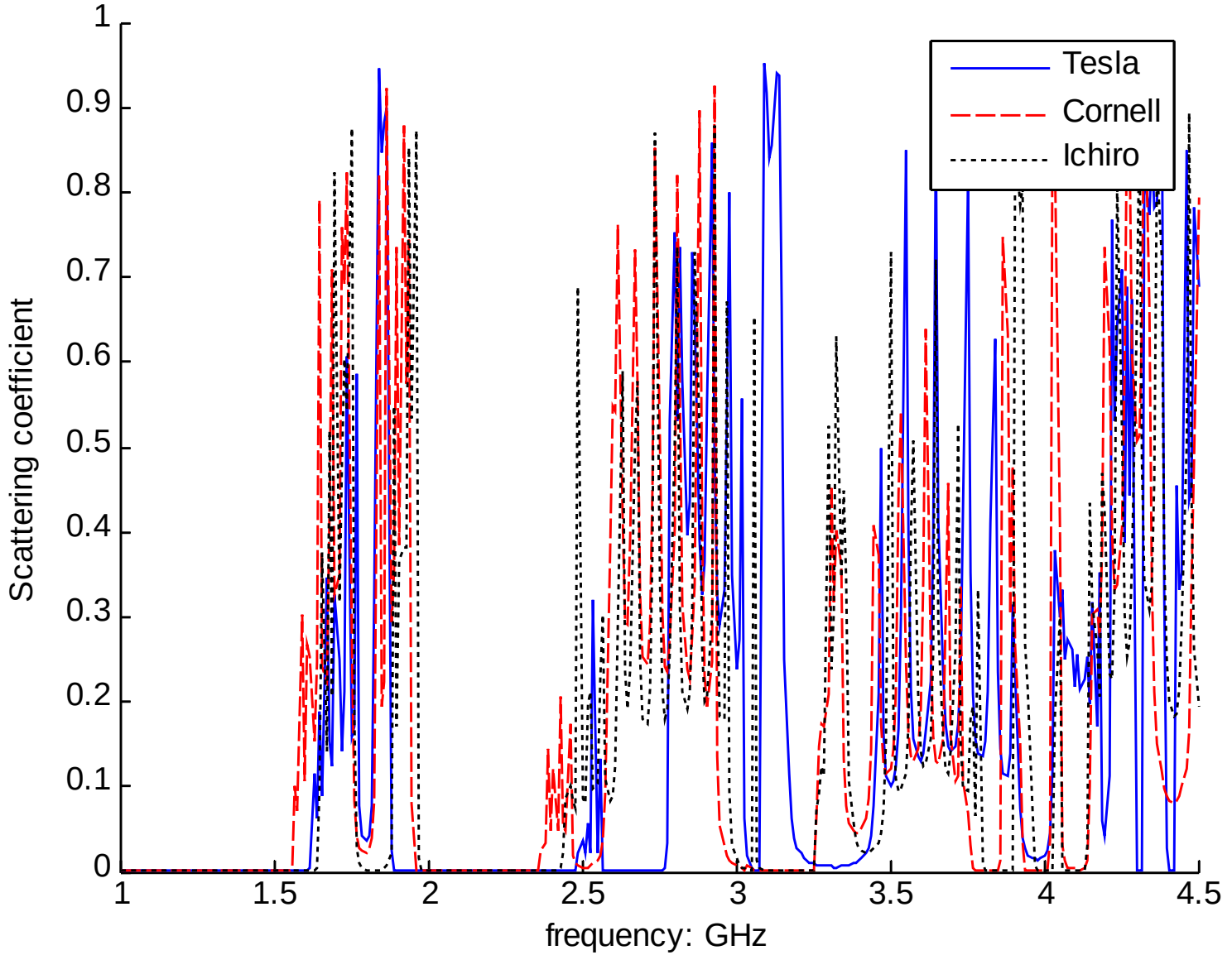

# Cascaded scattering matrix S21 of mode 1 as a function of mode 1 (TE11) in a complete Tesla Module

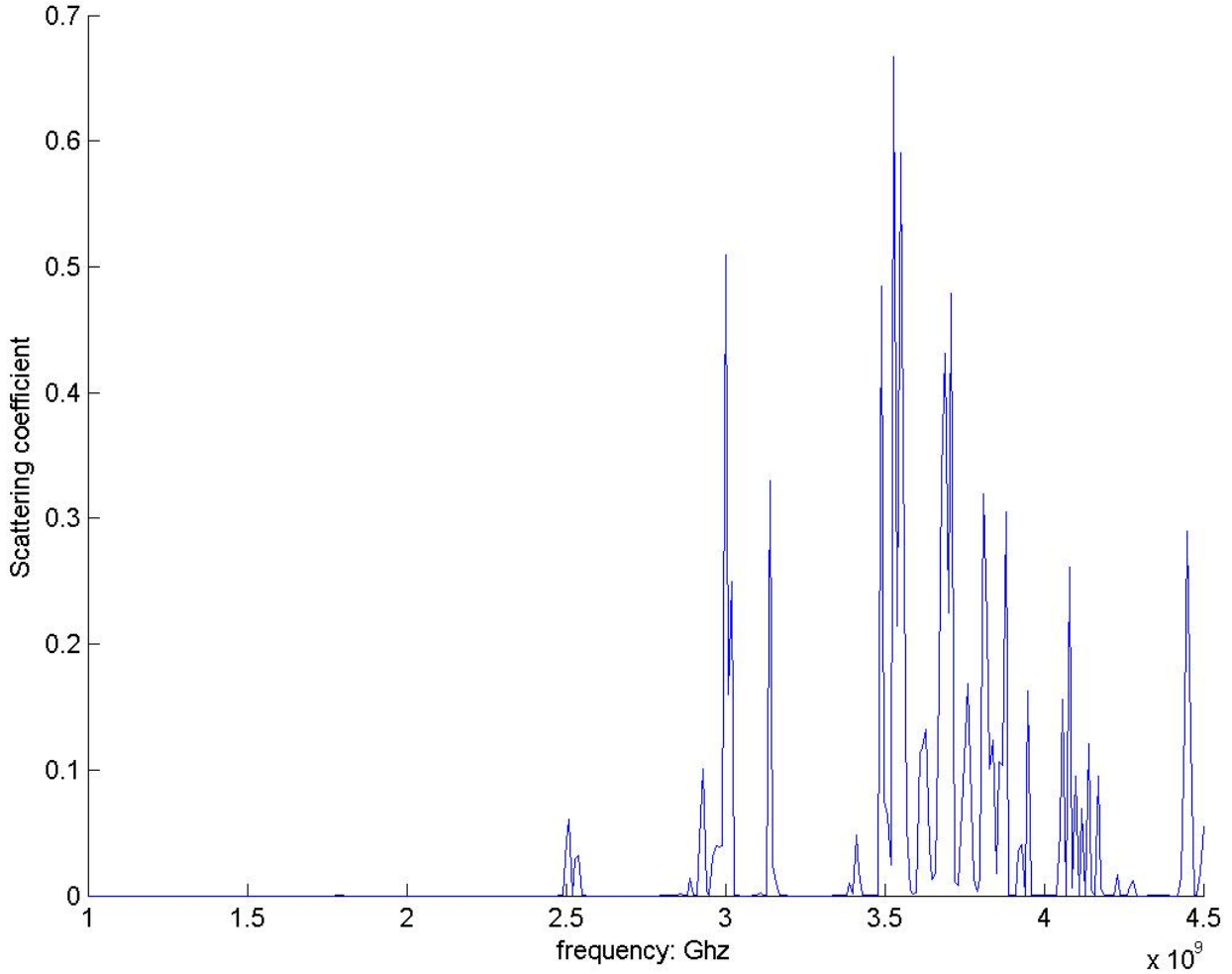

# Initial dented structure simulations

- An initial investigation was made into adding machining errors into the cascading scheme using a symmetrical dented perturbation
- Such perturbations could be used to shift potentially harmful trapped modes

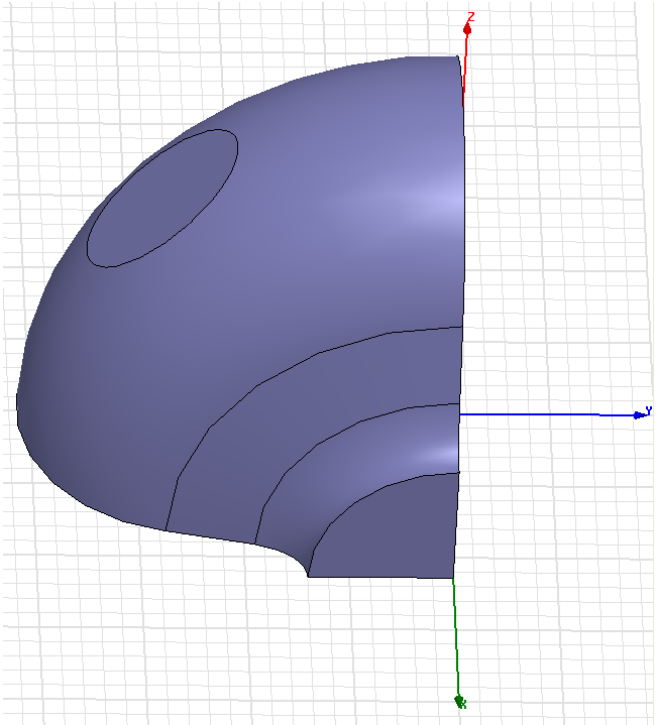

# Benchmarking against Slater's theorem

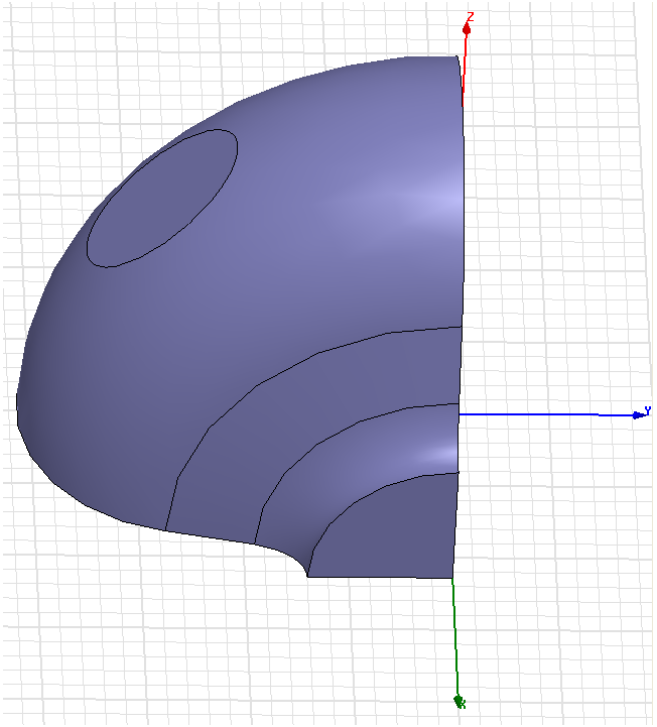

Slater's theorem consists of the combined perturbations of both the electric and magnetic boundaries – here due to the nature of the chosen perturbation only the electric field boundary condition needs to be considered hence Slater's theorem is reduced to:

$$f_{shift} = \frac{f_{unperturbed}}{\int ((\epsilon_0 E^2 + \mu_0 H^2)\partial V_{unperturbed})} x \int (\epsilon_0 E^2 + \mu_0 H^2)\partial V_{perturbed}$$

Slater's theorem is a good benchmarking technique, provided the perturbation itself does not significantly alter the modal structure. Benchmarked the symmetrical perturbation against Slater's theorem for a series of “Slices” for the three cavity designs of the TESLA, Cornell re-entrant and the Ichiro cavity.

# Initial dented study of the three cavity designs

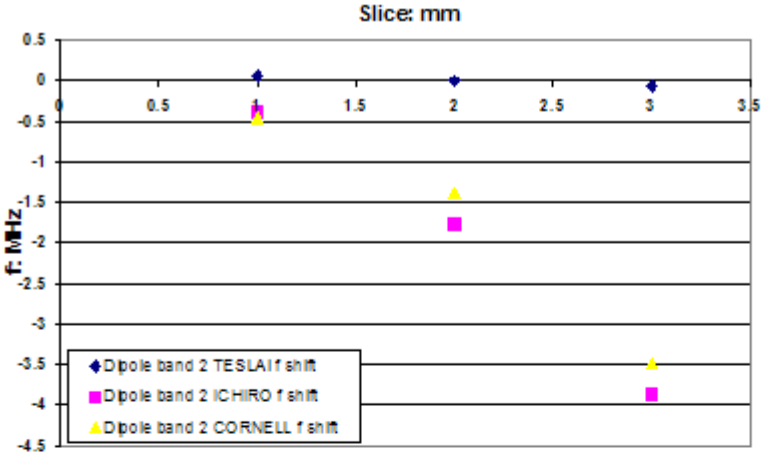


Graphical comparison of the three designs for frequency shifts as a function of slice size for the π phase mode of the second dipole band

| | TESLA | SLATER | TESLA | SLATER | TESLA | SLATER |
|---|---|---|---|---|---|---|
| Slice: mm | 1 | 1 | 2 | 2 | 3 | 3 |
| Dipole band 1 shift f0 | 0.05 | -0.01 | -0.15 | -0.05 | 0.08 | -0.10 |
| Dipole band 1 shift fpi | -0.22 | -0.25 | -1.13 | -1.24 | -2.84 | -2.47 |
| Dipole band 2 shift f0 | -0.39 | -0.37 | -1.76 | -1.59 | -3.97 | -3.28 |
| Dipole band 2 shift fpi | 0.06 | -0.01 | 0.00 | -0.05 | -0.07 | -0.10 |
| Dipole band 3 shift f0 | 0.28 | 0.10 | 0.64 | 0.42 | 1.33 | 0.86 |
| Dipole band 3 shift fpi | -0.04 | -0.13 | -0.18 | -0.65 | -0.98 | -1.28 |
| Dipole band 4 shift f0 | -0.01 | -0.13 | -0.57 | -0.57 | -1.49 | -1.22 |
| Dipole band 4 shift fpi | 0.46 | 0.21 | 1.20 | 0.96 | 1.86 | 1.76 |
| Sextupole band 1 shift f0 | 0.12 | -0.06 | -0.18 | -0.30 | -0.62 | -0.61 |
| Sextupole band 1 shift fpi | 0.21 | -0.05 | -0.13 | -0.28 | 0.17 | -0.42 |
| Sextupole band 2 shift f0 | -0.95 | -0.79 | -3.56 | -3.31 | -7.78 | -6.76 |
| Sextupole band 2 shift fpi | -0.90 | -0.69 | -3.44 | -3.33 | -7.90 | -6.63 |

Comparison between the numerically calculated frequency shifts in MHz and those calculated by Slaters theorem for various slice size perturbations applied at the equator radius for four symmetrically placed slices for 0 (F0) and π (Fpi) phase modes. Notable frequency shifts are highlighted in yellow. All results are accurate to ±0.5MHz.

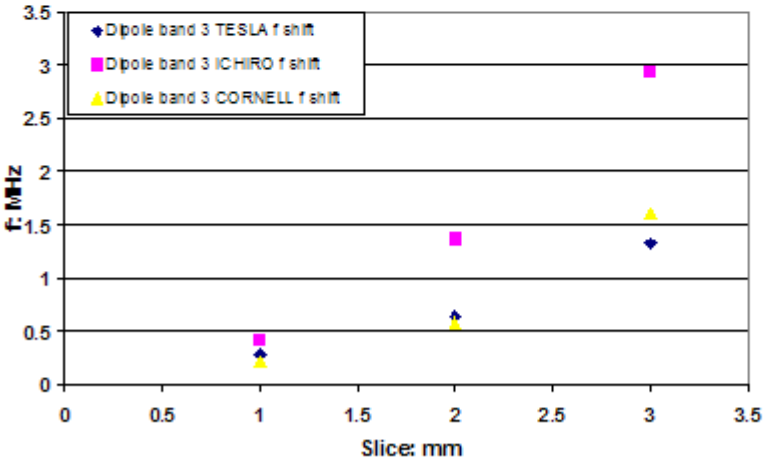


Graphical comparison of the three designs for frequency shifts as a function of slice size for the 0 phase mode of the third dipole band

| | TESLA | ICHIRO | CORNELL | TESLA | ICHIRO | CORNELL | TESLA | ICHIRO | CORNELL |
|---|---|---|---|---|---|---|---|---|---|
| Slice: mm | 1 | 1 | 1 | 2 | 2 | 2 | 3 | 3 | 3 |
| Dipole band 1 shift f0 | 0.05 | -0.05 | -0.01 | -0.15 | -0.01 | 0.07 | 0.08 | -0.09 | -0.31 |
| Dipole band 1 shift fpi | -0.22 | 0.05 | -0.09 | -1.13 | -0.05 | -0.17 | -2.84 | -0.18 | -0.33 |
| Dipole band 2 shift f0 | -0.39 | -0.45 | -0.35 | -1.76 | -2.12 | -1.56 | -3.97 | -4.73 | -4.25 |
| Dipole band 2 shift fpi | 0.06 | -0.39 | -0.46 | 0 | -1.77 | -1.38 | -0.07 | -3.87 | -3.48 |
| Dipole band 3 shift f0 | 0.28 | 0.42 | 0.21 | 0.64 | 1.37 | 0.58 | 1.33 | 2.94 | 1.61 |
| Dipole band 3 shift fpi | -0.04 | -0.56 | -0.17 | -0.18 | -0.84 | -0.31 | -0.98 | -1.6 | -0.91 |
| Dipole band 4 shift f0 | -0.01 | -0.45 | -0.21 | -0.57 | -1.86 | -1.31 | -1.49 | -4.04 | -3.61 |
| Dipole band 4 shift fpi | 0.46 | 0.03 | -0.44 | 1.2 | -0.6 | -0.99 | 1.86 | -1.91 | -1.78 |
| Sextupole band 1 shift f0 | 0.12 | -0.23 | -0.17 | -0.18 | -0.63 | -0.68 | -0.62 | -1.62 | -1.47 |
| Sextupole band 1 shift fpi | 0.21 | 0.81 | -0.24 | -0.13 | 1.85 | 0.65 | 0.17 | 3.97 | 2.21 |
| Sextupole band 2 shift f0 | -0.95 | -0.03 | 0.01 | -3.56 | -0.01 | 0.11 | -7.78 | -0.15 | -0.1 |
| Sextupole band 2 shift fpi | -0.9 | -0.43 | -0.61 | -3.44 | -2.48 | -1.93 | -7.9 | -5.48 | -5.07 |

Comparison of the numerically calculated frequency shifts in MHz for the three designs for various slice size perturbations applied at the equator radius for 0 (F0) and π (Fpi) phase modes. Notable frequency shifts are highlighted in yellow. All results are accurate to ±0.5MHz.

# Dented structures with a slice size of 5mm showing perturbation of the modes

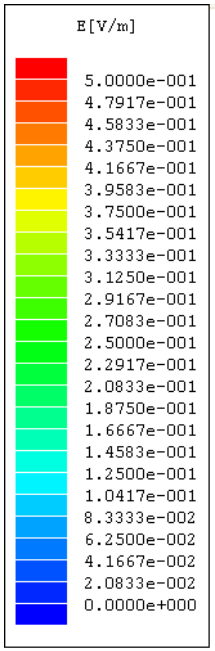


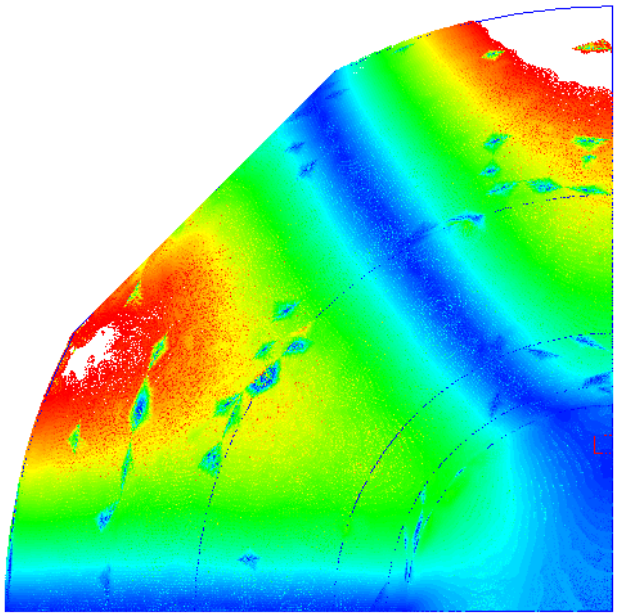

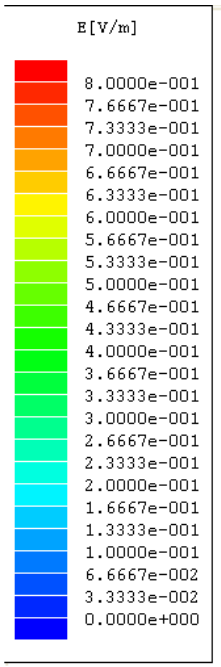


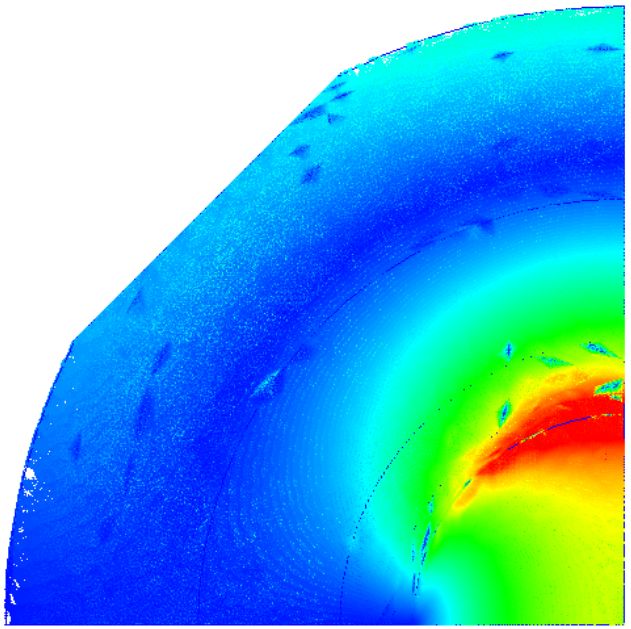

# Cascaded dented simulations

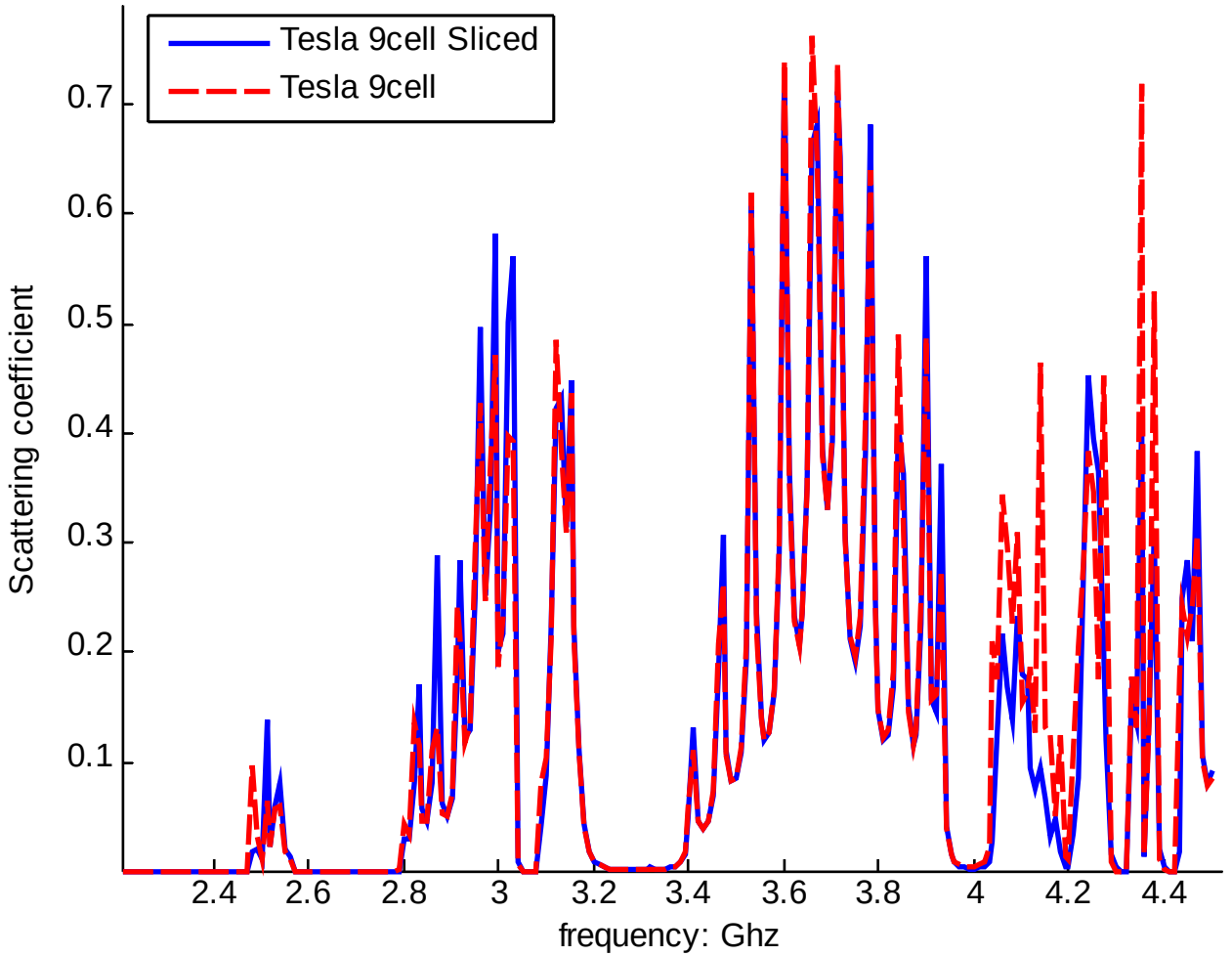


Zoomed in region of the generalised cascaded S21 matrix for a 9-cell TESLA structure comparison between an unperturbed structure and the RMS of a randomly perturbed structure for the TE11 mode scattered into the TE11 mode. Here the middle cells in the structure were randomly perturbed using slice sizes of 0mm, 1mm, 2mm and 3mm with the RMS taken for 20 different simulations.

# Further aspects of cascading a TESLA like structure with couplers

- With the inclusion of couplers a full 3D simulation without symmetry planes must be used – a lot of modes must be considered
- Unit cell considerations, use either: a 9cell 4port (or higher); a series of single cells; or a special 9cell unit structure?

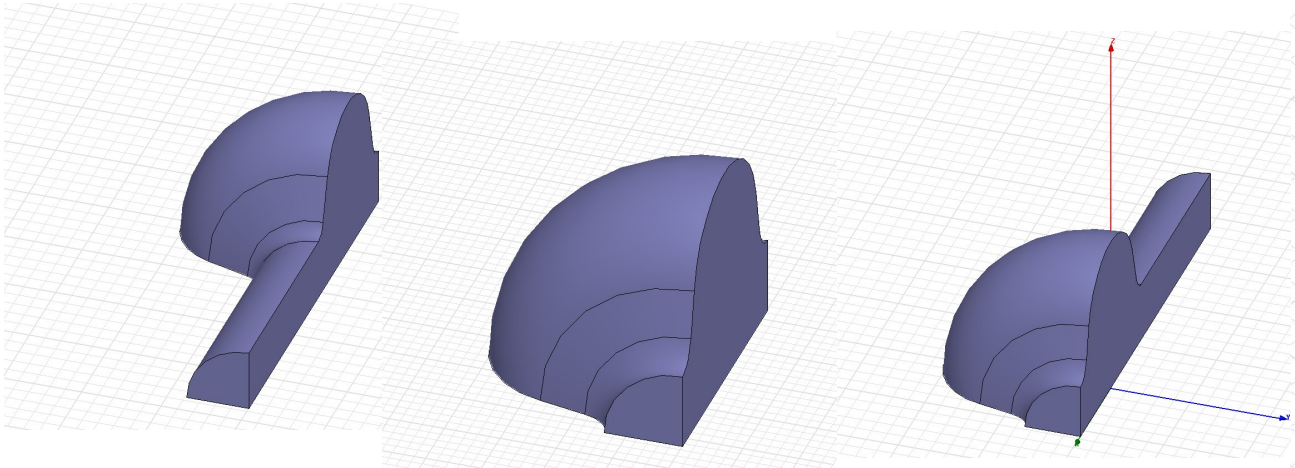

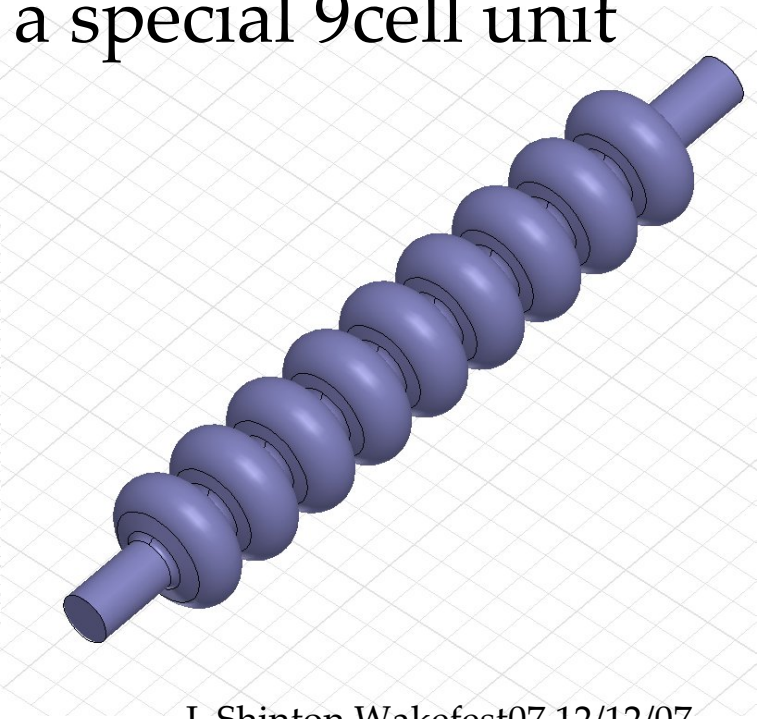

# Obtaining useful electromagnetic fields, kicks, R/Q's and wakefields from a cascading simulation

- By itself the GSM does not tell us a great deal
- The derivation of the electromagnetic fields from the GSM is what is required for useful design information: kicks, R/Q's, Wakefields etc.....
- There are a number of possibilities that could be used to calculate the electromagnetic field from the GSM:

1) Mode matching – computationally inexpensive; however care with the physics must be used.
2) Use the GSM as boundary conditions in a reworked driven modal solution – note this method would be computationally very expensive and time consuming.

# A mode matching approach using the GSM

A mode matching technique has been developed along the lines of:

J.Shmoys, R.M.Jones, B.R.Cheo, CEBAF-Report-89-001, pg 332-334

K.Rothemund, D.Hecht, U. van Rienen, Proceedings of LINAC 2004, pg 171-173

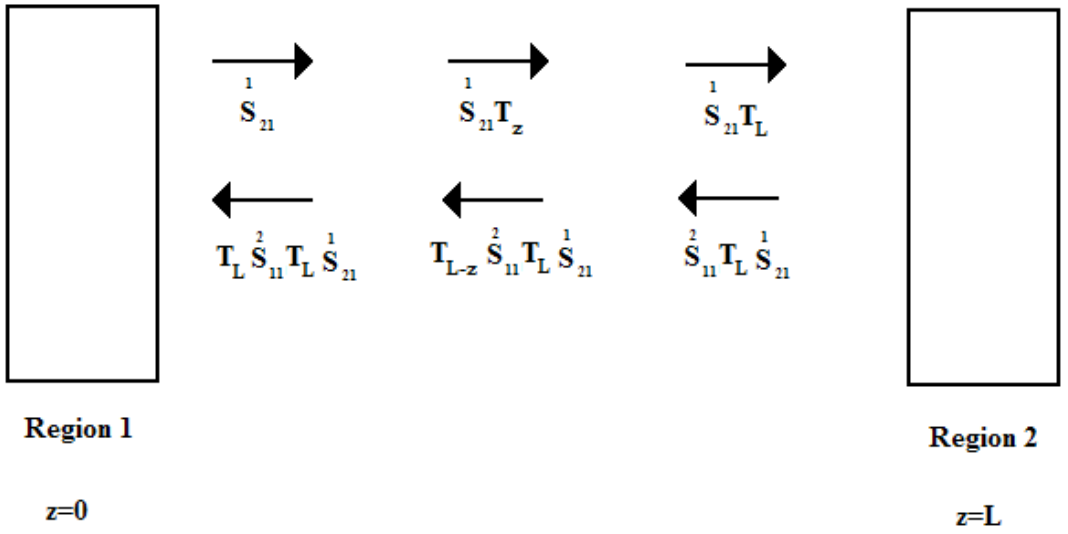


1) Derive a formula in terms of an infinite series
2) Using mode matching the formula can be condensed into the following form:

$$E_T = \sum_{1}^{N} e_n \left( T_z \overset{0}{S}_{21} - T_{-z} \overset{0}{S}_{11} \right)$$

$\overset{0}{S}_{11}$ and $\overset{0}{S}_{21}$ are special S matrices describing the infinite series in terms of regions 1 and 2, "T" is a diagonal matrix containing the exponential of propagation constant for the modes and "e" is the analytical field for a waveguide for a particular mode

3) Finally consider there to be a 0 gap length.

# Application of the initial mode matching technique

1) Consider the junctions between each of the unit cells in the structure and derive a GSM on each side of the junction i.e. cascade left and right of the junction
2) Obtain $\overset{0}{S}_{11}$ and $\overset{0}{S}_{21}$ (these are special S matrices that describe each side of the GSM junction – derived from the infinite series)
3) Use mode matching in terms of $\overset{0}{S}_{11}$ and $\overset{0}{S}_{21}$, the normalised field at the junction for any chosen mode can then be obtained.
4) This initial technique, used in conjunction with the overall GSM, can be used to give very quick indication of the electromagnetic field across a structure.

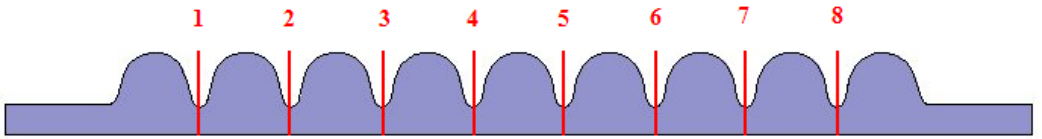

# A benchmarking example using a mode matching approach and the GSM

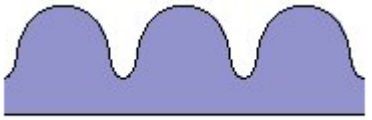

- Initial benchmark of mode matching scheme for a 3 cell structure against full simulation of HFSS
- The results in the table below show the typical error being between approximately 4% and 13%

| Frequency point : Ghz | Normalised HFSS complex magE Junction 1 | NormalisedCalculation Junction 1 | Normalised HFSS complex MagE Junction 2 | Normalised Calculation Junction 2 | % difference |
|---|---|---|---|---|---|
| 2.85 | 1 | 1 | 0.81 | 0.71 | 12.86 |
| 2.9 | 1 | 1 | 0.66 | 0.69 | 3.8 |

- In its current form this mode matching technique could be simply extended by taking a series of slices to get a fuller picture of the field across the structure – care needs to be taken in doing this.

# A quick look at the normalised fields at the junctions across all frequencies

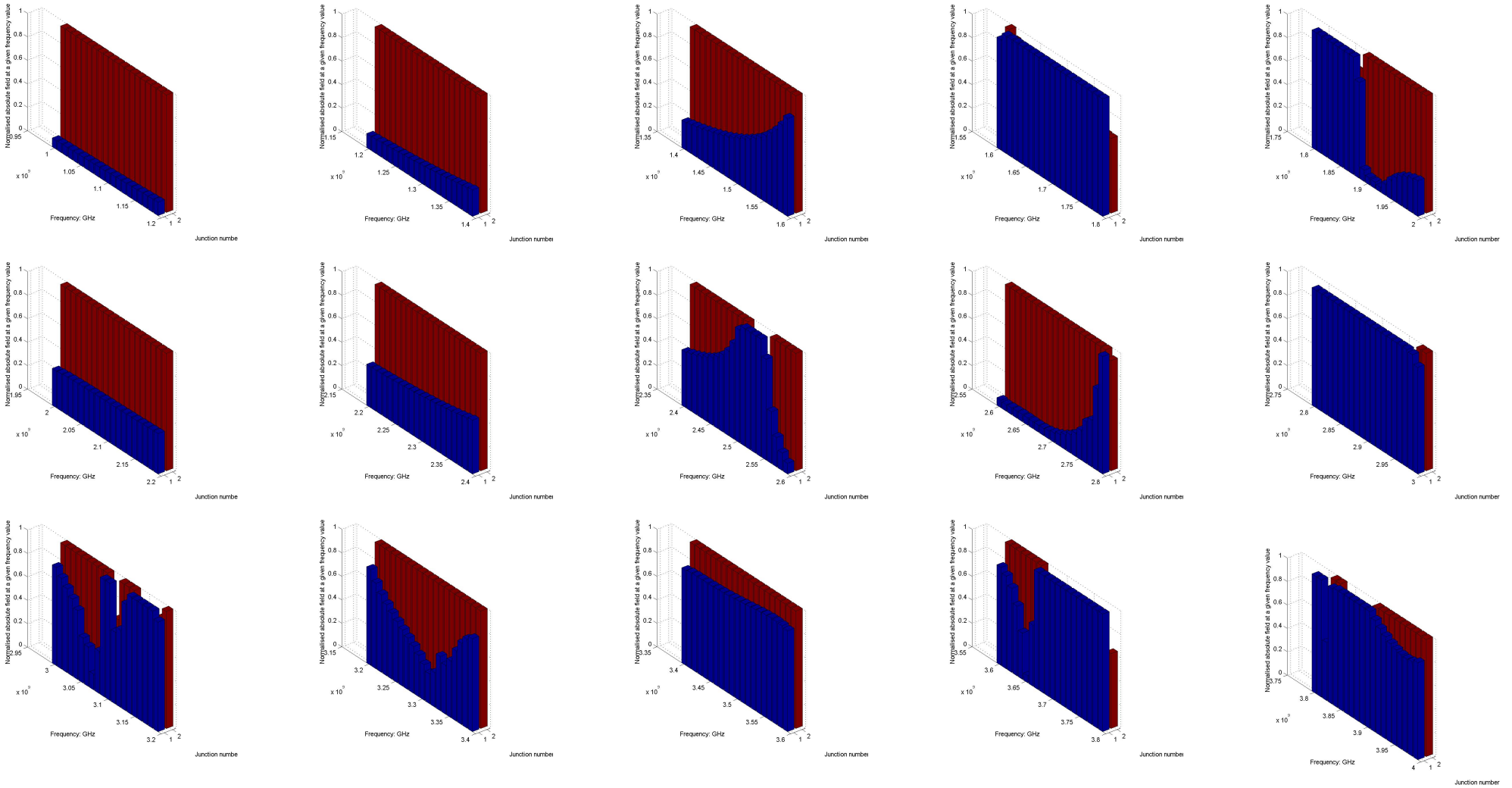

# Future work

1)The mode matching scheme as it is at the moment can be used as an initial design tool to look at the fields across an accelerating structure, this could be accomplished by extending the mode matching scheme using a propagation constant in which the radial dependence has been considered

2)Once the electromagnetic fields have been calculated the kick factors, R/Q's and finally Wakefields can be calculated.

# Summary

1) The generalised cascading technique is a proven RF technique that if used correctly produces the same results as a numerical scheme such as the FEM.

2) The generalised cascading technique requires little in the way of computational resources and is a very quick technique to apply to a large scale structure

3) The generalised cascading technique has the added bonus of being able to quickly (and simply) incorporate physical defects such as perturbations and cavity miss-alignments without the necessity to computationally re-mesh the structure

4) The mode matching electromagnetic field calculation presently under development is a useful design tool that can be used to quickly look at the general electromagnetic field of a structure across a large frequency range